

On the internal stability of non-linear dynamic inversion: application to flight control

ISSN 1751-8644
 Received on 15th August 2016
 Revised 21st March 2017
 Accepted on 31st March 2017
 E-First on 24th April 2017
 doi: 10.1049/iet-cta.2016.1067
 www.ietdl.org

Mushfiqul Alam¹ ✉, Sergej Celikovskiy²

¹Department of Measurement, Faculty of Electrical Engineering, Technicka 2, Czech Technical University in Prague, Prague, Czech Republic

²Institute of Information Theory and Automation, Czech Academy of Sciences, Pod Vodarenskou Vezi 4, CZ-182 08 Prague 8, Czech Republic

✉ E-mail: mushfala@fel.cvut.cz

Abstract: Aircraft are highly non-linear systems, but flight control laws are traditionally designed from a set of linearised models. Due to the application of linear control laws on a non-linear system, the real performance ability of the aircraft is not fully utilised. In addition, in adverse situations like near stall, the aircraft develops significant non-linearities, and linear control laws do not perform well. This study therefore considers the design of a longitudinal flight controller for a fixed-wing aircraft using non-linear dynamic inversion technique or, in terms of control theory, partial exact feedback linearisation. A novel contribution of this study is the proposed combination of three different automatic flight controllers that provide complete 3-DOF longitudinal control. A detailed analysis of the internal dynamics for each controller is also presented. It has been shown that for each controller the internal dynamics are stable. This makes the controller suitable for various flight conditions. The aims of these flight controllers are threefold. First, to provide control of the flight path angle by tracking the pitch angle and the angle of attack. Second, to provide high attitude (pitch up or down) manoeuvrability. Finally, to provide automatic adverse attitude recovery of the aircraft in situations like stall, the switching strategy between the controllers are also discussed. A simulation carried out on a non-linear model of a multi-role fighter aircraft verified the proposed theoretical results confirming the suitability of the controllers.

1 Introduction

The current state-of-the-art automatic flight control system (AFCS) provides efficient methods for pilots to fly the aircraft. The introduction of the fly-by-wire (FBW) system has enabled the aircraft to be stabilised automatically, preventing unsafe operation outside the performance envelope without input from the pilot [1]. However, in the critical conditions, where the aircraft gets outside the flight envelope the automatic flight control known as 'Autopilot' is disengaged, and the pilot is required to take manual corrective actions. An example of critical conditions of this kind is when the aircraft reaches critical angle of attack (or stall angle), beyond which the lift is suddenly reduced. This phenomenon is known as stall [2]. The standard stall recovery procedure (shown in Fig. 1) recommended in the pilot training is to push the control stick down, forcing a nose down motion of the aircraft. This makes the aircraft go faster and restores the required lift [3]. Pilots tend to misread the situation and take wrong corrective measure leading to an accident. A significant number of commercial and military air crash accidents have occurred after loss of control due to stalling caused by pilot error. Indonesia AirAsia Flight 8501, Air France Flight 447, Navy McDonnell-Douglas QF-4S+ Phantom II and United States Air Force Boeing C-17A Lot XII Globemaster III are some recent air accidents caused by pilot error and stall [4–7]. To address this problem, we propose three new different automatic flight controllers that can be used in different phases of flight based on the well-known partial exact feedback linearisation approach

within the realm of the non-linear dynamic inversion (NDI) technique.

Flight control laws below the stall angle are designed using linear control design methods such as gain scheduling [1]. The control laws are designed at many flight-operating points [8] and the gain scheduling is chosen as a function of mass, Mach number and altitude. This design procedure requires a great amount of assessment to ensure the adequate stability and performance at off-design points. It is time-consuming and the performance capabilities of the aircraft are not fully realised. As an alternative to gain scheduling robust control algorithms such as \mathcal{H}_2 and \mathcal{H}_∞ controllers are proposed [9]. However, at a large angle of attack (near the stall angle) aircraft develop significant non-linearities [10] and for this reason the linearised control laws do no longer hold. An alternative approach is to apply non-linear design techniques in critical flight conditions such as near stall point or high attitude angle (pitch angle) manoeuvres where the aircraft develops non-linearities. NDI directly make use of the non-linear structure of the aircraft model. It uses dynamic models and state feedback to globally linearise dynamics of selected controlled variables by cancelling the non-linearities in the dynamic model. As a result, the NDI method is capable of handling large non-linearities. NDI control law is designed to globally reduce the dynamics of selected controlled variables to integrators. A closed loop system is then designed to make the control variables exhibit specified command responses satisfying the flight-handling qualities and various physical limitation of the aircraft control

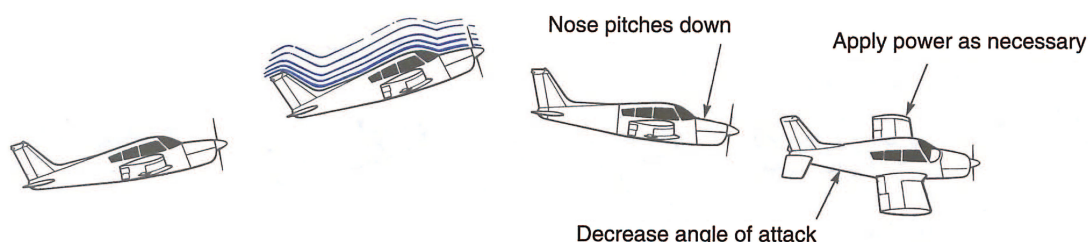


Fig. 1 Stall recovery procedure

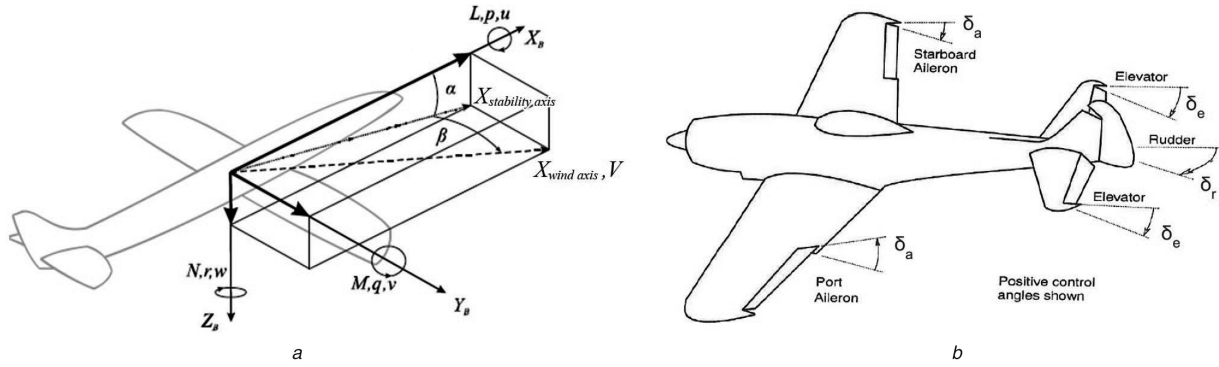


Fig. 2 Description of the aircraft system: V , flight path velocity; α , angle of attack; β , side-slip angle; ϕ, θ, ψ , Euler's angles; $\delta_e, \delta_a, \delta_r$, control surface deflections; F_T , engine thrust; p, q, r , angular rates; $I_{xx}, I_{yy}, I_{zz}, I_{xz}$, moments of inertia; L, M, N , aerodynamic moments; X_B, Y_B, Z_B , body forces

actuators. Flight control design using NDI was first proposed in the late 1970s [11, 12]. Since that time, a number of research efforts have been made to use non-linear control techniques for flight controls, e.g. as incremental NDI [13, 14], adaptive fuzzy sliding control [15, 16]. Various methods for analysing the robustness of the NDI flight controllers for a quasi-linear-parameter varying model were presented in [17, 18]. Stochastic robust non-linear control using control logic for a high incidence research concept aircraft is proposed in [19]. However, this work did not take the internal dynamics into account, and stability was limited to manual pilot inputs.

NDI is widely used for under-actuated mechanical systems [20]. Since the longitudinal dynamics of the aircraft is under-actuated, it is not possible to control all the states using a single controller. The novel approach presented here is a proposal for three different controllers corresponding to the output sets, which are angle of attack and pitch angle; velocity and pitch angle; finally, velocity and angle of attack. The first controller can be used for high pitch angle control for conditions like take-off while retaining control over the angle of attack. The second controller can be used as the pitch autopilot with control over the velocity. Finally, the third controller can be used for stall recovery of the aircraft at the same time preventing dangerous speed. A complete analysis of the internal dynamics for each controller is provided. The switching strategies between these three controllers are discussed. This approach with the use of NDI takes into account all significant non-linearities in the system utilising full performance capability of the aircraft. An original feature in this paper is the designing of the three flight controllers with a detailed outline of the stability of the internal dynamics.

This paper is organised as follows: Section 2 presents the dynamic model of the aircraft. Main results are given in Sections 3 and 4. Namely, Section 3 presents the detailed design of the control laws. Section 4 provides a detailed analysis of the simulation results. Section 5 contains the final concluding remarks.

2 Dynamic modeling

The aircraft configuration is illustrated in Fig. 2. For a conventional fixed-wing aircraft, the aerodynamic control surfaces that produce the moments are the horizontal tail (elevator), the ailerons and the vertical tail (rudder). Only two orientation angles relative to the wind, known as aerodynamic angles are needed to specify the aerodynamic forces and moments (angle of attack (α) and the side-slip angle (β)) acting on the aircraft [10].

2.1 Longitudinal aerodynamics

The aerodynamic forces (drag and lift) and the moment (pitching moment) acting on the aircraft are defined in terms of the non-dimensional aerodynamic coefficients ($C_{L_{Total}}, C_{D_{Total}}, C_{m_{Total}}$) are calculated as follows:

$$\begin{aligned} X_B &= \frac{1}{2} \rho V^2 S C_{D_{Total}} \\ M &= \frac{1}{2} \rho V^2 S c_{MAC} C_{m_{Total}} \\ Z_B &= \frac{1}{2} \rho V^2 S C_{L_{Total}} \end{aligned} \quad (1)$$

Here ρ denotes the air density, S denotes the aircraft's effective wing surface area, and c_{MAC} denotes the mean aerodynamic chord. The aerodynamic coefficients are specified as functions of aerodynamic angles, control surface deflections and the aerodynamic derivatives. Each component of the aerodynamic and moment coefficients is represented by a 'look up' table.

$$\begin{aligned} C_{L_{Total}} &= C_{L_0} + C_{L_\alpha} \alpha + C_{L_q} q \frac{c_{MAC}}{2V} + C_{L_{\delta_e}} \delta_e \\ &= C_L + C_{L_q} q \frac{c_{MAC}}{2V} + C_{L_{\delta_e}} \delta_e. \end{aligned} \quad (2)$$

$$\begin{aligned} C_{D_{Total}} &= C_{D_0} + C_{D_\alpha} \alpha^2 + C_{D_{\delta_e}} \delta_e \\ &= C_D + C_{D_{\delta_e}} \delta_e; \quad C_D \approx C_{D_0} + |C_{D_\alpha} \alpha^2|. \end{aligned} \quad (3)$$

$$\begin{aligned} C_{m_{Total}} &= C_{m_0} + C_{m_\alpha} \alpha + C_{m_q} q \frac{c_{MAC}}{2V} + C_{m_{\delta_e}} \delta_e \\ &= C_m + C_{m_q} q \frac{c_{MAC}}{2V} + C_{m_{\delta_e}} \delta_e. \end{aligned} \quad (4)$$

Here, subscripts stand for the aerodynamic derivative of the respective variables. The aerodynamic coefficients C_L, C_D and C_m are related to the lift, drag, and pitching moments produced by the main wing and are functions of angle of attack (α).

2.2 Rigid body equation of motion for the aircraft

The aerodynamic force and the moment models are combined with the vector equations of motion to obtain the aircraft dynamic motion model. The stability and the wind axes are treated as being fixed to frames that are rotating relative to the vehicle-body frame [10]. Combined with wind and body axes the total 3-DOF longitudinal dynamic motion of the aircraft is written as follows:

Force equations:

$$\begin{aligned} \dot{V} &= -\frac{X_B}{m} + \frac{F_T}{m} \cos \alpha \cos \beta \\ &\quad + g(\cos \phi \cos \theta \sin \alpha \cos \beta + \sin \phi \cos \theta \sin \beta - \sin \theta \cos \alpha \cos \beta). \end{aligned} \quad (5)$$

$$\begin{aligned} \dot{\alpha} &= -\frac{Z_B}{mV \cos \beta} + q - \tan \beta (p \cos \alpha + r \sin \alpha) \\ &\quad - \frac{F_T \sin \alpha}{mV \cos \beta} + \frac{g}{V \cos \beta} (\cos \phi \cos \theta \cos \alpha + \sin \theta \sin \alpha). \end{aligned} \quad (6)$$

Moment equation:

$$\dot{q} = \frac{(I_{zz} - I_{xx})}{I_{yy}} pr - \frac{I_{xz}}{I_{yy}}(p^2 - r^2) + \frac{M}{I_{yy}}. \quad (7)$$

Kinematic equation:

$$\dot{\theta} = q \cos \phi - r \sin \phi. \quad (8)$$

Assuming that the lateral-directional motion of the aircraft is independently and separately controlled bringing the aircraft to a wing-level flight condition the 3-DOF longitudinal model of the aircraft motion can be further simplified. The side-slip and roll angles are associated with the lateral dynamics, so it can be assumed that the roll angle (ϕ) and the side-slip angle (β) is zero. The 3-DOF longitudinal dynamics equation (5)–(8) get:

$$\dot{V} = -\frac{1}{2} \frac{\rho S}{m} (C_{D_0} + C_{D_\alpha}) V^2 - \frac{1}{2} \frac{\rho S}{m} C_{D_{\delta e}} (\alpha) V^2 \delta e + \frac{F_T \cos(\alpha)}{m} + g \sin(\alpha - \theta). \quad (9)$$

$$\dot{\alpha} = -\frac{1}{2} \frac{\rho S}{m} (C_{L_\alpha} + C_{L_\alpha}) V - \frac{1}{2} \frac{\rho S}{m} c_{MAC} C_{L_q} q - \frac{1}{2} \frac{\rho S}{m} C_{L_{\delta e}} V \delta e - \frac{\sin(\alpha) F_T}{mV} + q + \frac{g \cos(\alpha - \theta)}{V}. \quad (10)$$

$$\dot{q} = \frac{1}{2} \frac{\rho S}{I_{yy}} c_{MAC} (C_{m_0} + C_{m_\alpha}) V^2 + \frac{1}{4} \frac{\rho S}{I_{yy}} c_{MAC}^2 C_{m_q} V q + \frac{1}{2} \frac{\rho S}{I_{yy}} c_{MAC} V^2 C_{m_{\delta e}} \delta e. \quad (11)$$

$$\dot{\theta} = q. \quad (12)$$

3 Control law design

As has already been noted, we will study the case of simplified non-linear dynamics, namely the longitudinal model (9)–(12). This model has four state variables and two control inputs. First, let's put the equations into the standard state-space model form known in non-linear control theory [20]. Now, if we define the state variables as $[x_1, x_2, x_3, x_4]^T = [V, \alpha, q, \theta]^T$, and the control inputs as $[u_1, u_2]^T = [\delta e, F_T]^T$, then the system in (9)–(12) can be written in the following form: (see (13))

Here, $x \in \mathbb{R}^4$, $u \in \mathbb{R}^2$, $f(x) = (f_i(x)) \in \mathbb{R}^4$, and $g(x) = (g_{ij}(x)) \in \mathbb{R}^{4 \times 2}$, where $i = 1, 2, 3, 4$ and $j = 1, 2$.

Furthermore, lets denote $g^j = [g_{1j}, g_{2j}, g_{3j}, g_{4j}]^T$, $j = 1, 2$, and $b_1 = -\frac{\rho S}{2m}$; $b_2 = b_1 C_{D_{\delta e}}$; $b_5 = C_{L_0}$; $b_6 = b_1 c_{MAC} C_{L_q}$; $b_7 = b_1 C_{L_{\delta e}}$; $b_8 = \frac{\rho S}{2I_{yy}} c_{MAC}$; $b_9 = b_8 c_{MAC} C_{m_q}$; $b_{10} = b_8 C_{m_{\delta e}}$; $b_3 = \frac{1}{m}$; $b_4 = g$; $b_{11} = C_{D_0}$; $b_{12} = C_{D_\alpha}$; $b_{13} = C_{L_\alpha}$; $b_{14} = C_{m_0}$; $b_{15} = C_{m_\alpha}$. Moreover, $C_{L_{\delta e}}, C_{L_q}, C_{L_\alpha}, C_{D_0} > 0$ and $C_{m_q}, C_{m_{\delta e}}, C_{m_\alpha} < 0$. Thus the variables $b_1, b_2, b_6, b_7, b_9, b_{10} < 0$ and $b_3, b_4, b_5, b_8, b_{11}, b_{13} > 0$.

To compute partial exact feedback linearisation of (13), the notion of the so-called auxiliary/virtual output is used. Namely, by defining a suitable output functions $h(x) = [h_1(x), h_2(x)]^T$, $x \in \mathbb{R}^4$ we can compute the input–output linearisation transforming certain sub-systems to linear form. To proceed with, $h(x)$ is said to have

vector relative degree $r = (r^1, r^2)$ around some equilibrium working point $x_o \in \mathbb{R}^4$ if r^1, r^2 is the integers such that there exists neighbourhood of x_o denoted as N_{x_o} , it holds:

$$\mathcal{L}_g^l \mathcal{L}_f^k h(x) \equiv 0, \quad x \in N_{x_o}, \quad k, j = 1, 2, \quad l = 0, \dots, r^k - 2 \quad (14)$$

$$\text{rank} \left[\mathcal{L}_g^l \mathcal{L}_f^{(r^k-1)} h(x_o) \right] = 2, \quad k, j = 1, 2. \quad (15)$$

Here, \mathcal{L}_f^m , $m = 0, 1, \dots$, stands for the so-called Lie derivatives and their iterations [20]. More precisely:

$$\mathcal{L}_f h = \nabla h f, \quad \nabla h = \frac{\partial h}{\partial x},$$

$$\mathcal{L}_f^0 h = h, \quad \mathcal{L}_f^m h = \mathcal{L}_f(\mathcal{L}_f^{m-1} h) = \nabla(\mathcal{L}_f^{m-1} h) f, \quad m = 1, 2, 3, \dots$$

It is well-known [20] that the n -dimensional system with vector relative degree $r = (r^1, r^2) \geq 1$ has $(r^1 + r^2)$ -dimensional exact feedback linearisable part has $n - (r^1 + r^2)$ residual non-linear part. The residual part of the system dynamics is called ‘internal dynamics’. It is important to ensure that the internal dynamics of the residual part or state that is left uncontrolled is stable. The autonomous part which keeps the selected output zero is referred to as the zero-dynamics. In the following sections, we will present three different selections of pairs of outputs giving three different partial linearisations (three different controllers) and their internal dynamics analysis.

3.1 Flight controller for angle of attack and pitch angle (flight controller no. 1)

This flight controller is to be used for situations like take-off where the primary focus is on lifting the aircraft with a desired pitch angle ($\theta = x_4$) at a certain take-off speed and to have a control over the angle of attack ($\alpha = x_2$), so that the aircraft has enough lift to get off the ground without stalling. Following (13) the relation between the pitch rate ($q = x_3$) and the pitch angle ($\theta = x_4$) is a single integrator, so x_4 can be tracked jointly with x_3 .

3.1.1 Control design.: The control objective for this controller is to design a tracking controller for x_2 and x_4 while stabilising the x_3 . Thus the auxiliary outputs chosen to get the partial exact feedback linearisation for Flight Controller No. 1, denoted as $h^1(x)$ are as follows:

$$h^1(x) = \begin{bmatrix} x_2 \\ x_4 \end{bmatrix}.$$

Let the virtual inputs to stabilise \dot{x}_3 be v_1 and to control \dot{x}_2 be v_2 . Lie derivative computation of $h^1(x)$ following (14) and (15) show that it has relative degrees $r = (1, 2)$. This allows us to obtain the feedback linearised form of the system (13) as

$$\begin{aligned} \dot{x}_2 &= v_2, \\ \dot{x}_3 &= v_1, \\ \dot{x}_4 &= x_3. \end{aligned}$$

$$\begin{bmatrix} \dot{x}_1 \\ \dot{x}_2 \\ \dot{x}_3 \\ \dot{x}_4 \end{bmatrix} = \begin{bmatrix} b_1 b_{11} x_1^2 + b_1 b_{12} x_2 x_1^2 + b_4 \sin(x_2 - x_4) \\ b_1 b_5 x_1 + b_1 b_{13} x_2 x_1 + b_6 x_3 + x_3 + b_4 x_1^{-1} \cos(x_2 - x_4) \\ b_8 b_{14} x_1^2 + b_8 b_{15} x_2 x_1^2 + b_9 x_1 x_3 \\ x_3 \end{bmatrix} + \begin{bmatrix} b_2 x_1^2 & b_3 \cos(x_2) \\ b_7 x_1 & -b_3 x_1^{-1} \sin(x_2) \\ b_{10} x_1^2 & 0 \\ 0 & 0 \end{bmatrix} \begin{bmatrix} u_1 \\ u_2 \end{bmatrix}. \quad (13)$$

Now the virtual inputs v_1 and v_2 are defined as follows:

$$\begin{bmatrix} v_1 \\ v_2 \end{bmatrix} = \begin{bmatrix} f_3 \\ f_2 \end{bmatrix} + \begin{bmatrix} g_{31} & 0 \\ g_{21} & g_{22} \end{bmatrix} \begin{bmatrix} u_1 \\ u_2 \end{bmatrix}. \quad (16)$$

The conditions for the existence of the relative degree as mentioned in (14) and (15) hold if and only if $x_1 \neq 0$ and $x_2 \neq l\pi$, l is an integer. This does not limit the applicability of the designed controller as x_1 is the velocity and x_2 is the angle of attack while lifting the aircraft which always occurs with non-zero angle of attack. Following (16) the input equations for u_1 and u_2 can be rewritten as follows:

$$\begin{bmatrix} u_1 \\ u_2 \end{bmatrix} = \begin{bmatrix} g_{31} & 0 \\ g_{21} & g_{22} \end{bmatrix}^{-1} \begin{bmatrix} -f_3 \\ -f_2 \end{bmatrix} + \begin{bmatrix} v_1 \\ v_2 \end{bmatrix}, \quad (17)$$

$$u_1 = \frac{-(b_8 b_{14} x_1^2 + b_8 b_{15} x_2 x_1^2 + b_9 x_1 x_3) + v_1}{b_{10} x_1^2}. \quad (17)$$

$$u_2 = \frac{-(b_1 b_5 x_1 + b_1 b_{13} x_2 x_1 + b_6 x_3 + x_3 + b_4 x_1^{-1} \cos(x_2 - x_4)) b_{10} x_1^2}{(b_{10} x_1^2)(-b_3 x_1^{-1} \sin x_2)} + \frac{(b_8 b_{14} x_1^2 + b_8 b_{15} x_2 x_1^2 + b_9 x_1 x_3) b_7 x_1}{(b_{10} x_1^2)(-b_3 x_1^{-1} \sin x_2)} + \frac{-b_7 x_1 v_1 + b_{10} x_1^2 v_2}{(b_{10} x_1^2)(-b_3 x_1^{-1} \sin x_2)}. \quad (18)$$

Further, consider the subsystem involving x_3, x_4 and the virtual input v_1 . This is a system with a double integrator relationship. To track some reference $x_3^{\text{ref}}(t), x_4^{\text{ref}}(t)$, have in mind that it should hold $x_3^{\text{ref}} = \dot{x}_4^{\text{ref}}$. Now to track the references, let us define the tracking error as follows:

$$e_3 = x_3 - \dot{x}_4^{\text{ref}}, \quad \dot{e}_3 = \dot{x}_3 - \ddot{x}_4^{\text{ref}}, \quad (19)$$

$$e_4 = x_4 - x_4^{\text{ref}}, \quad \dot{e}_4 = \dot{x}_4 - \dot{x}_4^{\text{ref}} = e_3. \quad (20)$$

The feedback tracking controller equation for x_3 can be written as

$$\dot{x}_3 = v_1 = \ddot{x}_4^{\text{ref}} + k_3(x_3 - \dot{x}_4^{\text{ref}}) + k_4(x_4 - x_4^{\text{ref}}). \quad (21)$$

Here k_3 and k_4 are the feedback control gains. Using (19)–(21) we get:

$$\dot{e}_3 = k_3 e_3 + k_4 e_4; \quad \dot{e}_4 = e_3. \quad (22)$$

Therefore, choosing $k_3 < 0$ and $k_4 < 0$, we get $e_3 \rightarrow 0$ and $e_4 \rightarrow 0$ exponentially, which means that exponential tracking is achievable.

Consider the subsystem involving x_2 and the virtual input v_2 . This system is directly related as a single integrator. We assume $x_2^{\text{ref}}(t)$ is to be tracked and we define tracking error e_2 as

$$e_2 = x_2 - x_2^{\text{ref}}, \quad \dot{e}_2 = \dot{x}_2 - \dot{x}_2^{\text{ref}}. \quad (23)$$

The feedback tracking controller for x_2 can be written in the form:

$$\dot{x}_2 = v_2 = \dot{x}_2^{\text{ref}} + k_2(x_2 - x_2^{\text{ref}}). \quad (24)$$

Here k_2 is the feedback tracking control gain. Now, combining (23) and (24) gives

$$\dot{e}_2 = k_2 e_2.$$

By choosing $k_2 < 0$, $e_2 \rightarrow 0$, hence exponential tracking is possible for the reference angle of attack x_2^{ref} . Substituting (21) and (24) into (17) and (18) gives the complete closed form expression for u_1 and u_2 as (see (25))

(see (26))

Combining the two controllers enables us to control both the pitch angle x_4 and the angle of attack x_2 , provided that the corresponding internal non-linear residual dynamics of the velocity x_1 has favourable properties.

3.1.2 Internal dynamics of the velocity (x_1): During the design of the controller the velocity x_1 is left uncontrolled. This corresponds to the hidden uncontrolled internal dynamics. It is essential to check and ensure that the internal dynamics of the velocity is stable. To check the stability of the internal dynamics, substitute the expression of control input u_1 and u_2 (25) and (26) into the equation of \dot{x}_1 in (13). For simplicity zero-dynamics are studied, hence for reference tracking $x_2^{\text{ref}}(t), x_4^{\text{ref}}(t), x_3^{\text{ref}}(t)$ the virtual inputs $v_1 = v_2 = 0$. For the purposes of the analysis constant reference tracking is considered. This means $x_2^{\text{ref}} \equiv x_2^e, x_4^{\text{ref}} \equiv x_4^e, \dot{x}_3^{\text{ref}} \equiv 0$, here x_2^e and x_4^e are constant and therefore we have to analyze stability of the equilibrium of the one dimensional velocity internal dynamics given by

$$\dot{x}_1 = \bar{f}_1(x_1),$$

Here $\bar{f}_1(x_1)$ is given by (51) derived in Appendix 1. To analyse the stability, we have to first compute the equilibrium velocity by solving (52) and then to analyse the Jacobian of $\bar{f}_1(x_1)$ at x_1^e , i.e. $(\partial \bar{f}_1 / \partial x_1)(x_1^e)$. We will show that $(\partial \bar{f}_1 / \partial x_1)(x_1^e) < 0$ and therefore by the first method of Lyapunov x_1^e is the locally exponentially stable equilibrium of (51). To be more specific, rewrite (52) as follows:

$$0 = ((x_1^e)^2) \left[\cot(x_2^e) \left(b_1 b_5 - \frac{b_7 b_8 b_{14}}{b_{10}} \right) + x_2^e \cot(x_2^e) \left(b_1 b_{13} - \frac{b_7 b_8 b_{15}}{b_{10}} \right) + b_1 b_{11} + b_1 b_{12} x_2^e \right] + \left[b_4 \cot(x_2^e) \cos(x_2^e - x_4^e) - \frac{b_2}{b_{10}} (b_2 b_{14} + b_8 b_{15} x_2^e) + b_4 \sin(x_2^e - x_4^e) \right], \quad (27)$$

here x_2^e, x_4^e are given required reference angle of attack and pitch angle and x_1^e is the velocity to be determined. Equation (27) is obviously a simple quadratic equation of the form $A(x_1^e)^2 + B = 0$.

$$u_1 = \frac{-(b_8 b_{14} x_1^2 + b_8 b_{15} x_2 x_1^2 + b_9 x_1 x_3) + \ddot{x}_4^{\text{ref}} + k_3(x_3 - \dot{x}_4^{\text{ref}}) + k_4(x_4 - x_4^{\text{ref}})}{b_{10} x_1^2}. \quad (25)$$

$$u_2 = \frac{-(b_1 b_5 x_1 + b_1 b_{13} x_2 x_1 + b_6 x_3 + x_3 + b_4 x_1^{-1} \cos(x_2 - x_4)) b_{10} x_1^2 + (b_8 b_{14} x_1^2 + b_8 b_{15} x_2 x_1^2 + b_9 x_1 x_3) b_7 x_1}{(b_{10} x_1^2)(-b_3 x_1^{-1} \sin x_2)} + \frac{(\dot{x}_2^{\text{ref}} + k_2(x_2 - x_2^{\text{ref}})) b_{10} x_1^2 - b_7 x_1 (\ddot{x}_4^{\text{ref}} + k_3(x_3 - \dot{x}_4^{\text{ref}}) + k_4(x_4 - x_4^{\text{ref}}))}{(b_{10} x_1^2)(-b_3 x_1^{-1} \sin x_2)}. \quad (26)$$

The coefficient of $(x_1^e)^2$ is $A = \cot(x_2^e)[(b_1b_5 - (b_7b_8b_{14}/b_{10})) + x_2^e(b_1b_{13} - (b_7b_8b_{15}/b_{10}))] + b_1b_{11} + b_1b_{12}x_2^e$ and $B = [b_4\cot(x_2^e)\cos(x_2^e - x_4^e) - (b_2/b_{10})(b_2b_{14} + b_8b_{15}x_2^e) + b_4\sin(x_2^e - x_4^e)]$.

Consider the term A, here $\cot(x_2^e)[(b_1b_5 - (b_7b_8b_{14}/b_{10})) + x_2^e(b_1b_{13} - (b_7b_8b_{15}/b_{10}))]$ is associated with the lift. Here by definition, for $x_2^e > 0$, the lift produced is considered to be negative (by convention), hence $(b_1b_5 - (b_7b_8b_{14}/b_{10})) + x_2^e(b_1b_{13} - (b_7b_8b_{15}/b_{10})) < 0$. In addition when $x_2^e > 0$, $\cot(x_2^e) > 0$ and $x_2^e < 0$, $\cot(x_2^e) < 0$. Also the term $(b_1b_{11} + b_1b_{12}x_2^e)$ is associated with drag and by definition it is always negative. This implies that the coefficient of $(x_1^e)^2$ is always negative.

Now consider the term B. Here the term $(b_2/b_{10})(b_2b_{14} + b_8b_{15}x_2^e)$ is associated with the coefficient of pitching moment. Hence for $x_2^e > 0$, $(b_2/b_{10})(b_2b_{14} + b_8b_{15}x_2^e) > 0$ and $x_2^e < 0$, $(b_2/b_{10})(b_2b_{14} + b_8b_{15}x_2^e) < 0$. Therefore for B to be positive, it is necessary to satisfy that

$$\cos(x_2^e - x_4^e) + \sin(x_2^e - x_4^e) > 0. \quad (28)$$

From (28), it can be said that for every combination of x_2^e and x_4^e B is positive. Hence, it can be concluded that for every selection of x_2^e , x_4^e (27) can be solved to find a unique equilibrium velocity x_1^e .

To study the local stability of (27) its linear approximation around the selected equilibrium points $x = (x_1^e, x_2^e, 0, x_4^e)$ is considered. Thus the partial derivative of (27) (Jacobian) becomes:

$$\begin{aligned} \dot{x}_1 = & [2x_1^e\cot(x_2^e)(b_1b_5 + b_1b_{13}x_2^e) - \frac{2b_2x_1^e}{b_{10}}(b_8b_{14} + b_8b_{15}x_2^e) + \\ & - \frac{b_7\cot(x_2^e)x_1^e}{b_{10}}(b_8b_{14} + b_8b_{15}x_2^e)][x_1 - x_1^e] + \mathcal{O}[x_1 - x_1^e]. \end{aligned} \quad (29)$$

The simplified Jacobian (J_{x1}) from (29) can be written as

$$\begin{aligned} J_{x1} = & x_1^e \left[2\cot(x_2^e)(b_1b_5 + b_1b_{13}x_2^e) + 2(b_1b_{11} + b_1b_{12}x_2^e) \right. \\ & \left. + \left(-\frac{2b_2}{b_{10}} - \frac{b_7\cot(x_2^e)}{b_{10}} \right) (b_8b_{14} + b_8b_{15}x_2^e) \right]. \end{aligned} \quad (30)$$

Following (30), it can be seen that for $x_2^e > 0$ or $x_2^e < 0$ the terms $2\cot(x_2^e)(b_1b_5 + b_1b_{13}x_2^e) < 0$ and $2(b_1b_{11} + b_1b_{12}x_2^e) < 0$. For $x_2^e > 0$ the term $\left(-\frac{2b_2}{b_{10}} - \frac{b_7\cot(x_2^e)}{b_{10}} \right) (b_8b_{14} + b_8b_{15}x_2^e) > 0$ and for $x_2^e < 0$, $\left(-\frac{2b_2}{b_{10}} - \frac{b_7\cot(x_2^e)}{b_{10}} \right) (b_8b_{14} + b_8b_{15}x_2^e) < 0$. Also

$$\begin{aligned} & |2\cot(x_2^e)(b_1b_5 + b_1b_{13}x_2^e) + 2(b_1b_{11} + b_1b_{12}x_2^e)| \\ & \gg \left| \left(-\frac{2b_2}{b_{10}} - \frac{b_7\cot(x_2^e)}{b_{10}} \right) (b_8b_{14} + b_8b_{15}x_2^e) \right|. \end{aligned}$$

Thus it holds that the term J_{x1} in (30) is always negative. Therefore linear approximation in (29) takes the form:

$$\dot{x}_1 = \tau x_1^e (x_1 - x_1^e).$$

Here,

$$\begin{aligned} \tau = & \left[2\cot(x_2^e)(b_1b_5 + b_1b_{13}x_2^e) + 2(b_1b_{11} + b_1b_{12}x_2^e) \right. \\ & \left. + \left(-\frac{2b_2}{b_{10}} - \frac{b_7\cot(x_2^e)}{b_{10}} \right) (b_8b_{14} + b_8b_{15}x_2^e) \right] < 0. \end{aligned}$$

This confirms that any positive equilibrium velocity x_1^e is exponentially stable, i.e. the zero-dynamics of the controller is exponentially stable. It should be noted that the value of τ is small. Therefore, during tracking the target values of pitch angle and angle of attack, the change in the velocity will not be very fast or rapid. It can be noted that flight path angle $\gamma = x_4 - x_2$, so by choosing appropriate angle of the attack and pitch angle, flight path angle can be controlled.

3.2 Flight controller for pitch angle and velocity (Flight Controller No. 2)

This flight controller can be used for pitch angle (x_4) control while maintaining or tracking a certain desired velocity (x_1), when, e.g. during the cruising or steady climb. In this controller, x_4 is controlled using the elevator deflection (u_1) and x_1 is controlled by the engine throttle (u_2).

3.2.1 Control design.: The control objective for this controller is to design a tracking controller for x_1 and x_4 . Thus the auxiliary outputs chosen to get the partial exact feedback linearisation for Flight Controller No. 2, denoted as $h^2(x)$ are as follows:

$$h^2(x) = \begin{bmatrix} x_1 \\ x_4 \end{bmatrix}.$$

Let the virtual inputs to stabilise \dot{x}_3 be v_1 and to control \dot{x}_1 be v_2 . Lie derivative computation of $h^2(x)$ following (14) and (15) shows that the relative degrees $r = (1, 2)$. This allows us to obtain the feedback linearised form of the system (13) as

$$\begin{aligned} \dot{x}_1 &= v_2, \\ \dot{x}_3 &= v_1, \\ \dot{x}_4 &= x_3. \end{aligned}$$

The virtual inputs v_1 and v_2 are defined as follows:

$$\begin{bmatrix} v_1 \\ v_2 \end{bmatrix} = \begin{bmatrix} f_3 \\ f_1 \end{bmatrix} + \begin{bmatrix} g_{31} & 0 \\ g_{11} & g_{12} \end{bmatrix} \begin{bmatrix} u_1 \\ u_2 \end{bmatrix}. \quad (31)$$

The conditions for the existence of the relative degree as mentioned in (14) and (15) hold if and only if $x_1 \neq 0$ and $x_2 \neq (l/2)\pi$, l is an integer. Therefore, in the control design we consider the aircraft is in some state where $x_1 \neq 0$, $x_2 \neq (l/2)\pi$. These conditions are satisfied in all real flight conditions because the aircraft velocity can never be zero and the angle of attack cannot be $(l/2)\pi$. Following (31) the input equations for u_1 and u_2 can be rewritten as follows:

$$\begin{aligned} \begin{bmatrix} u_1 \\ u_2 \end{bmatrix} &= \begin{bmatrix} g_{31} & 0 \\ g_{11} & g_{12} \end{bmatrix}^{-1} \begin{bmatrix} f_3 \\ f_1 \end{bmatrix} + \begin{bmatrix} v_1 \\ v_2 \end{bmatrix}. \\ u_1 &= \frac{-(b_8b_{14}x_1^2 + b_8b_{15}x_2x_1^2 + b_9x_1x_3) + v_1}{b_{10}x_1^2}. \end{aligned} \quad (32)$$

(see (33))

The complete closed form expression for u_2 is given as (see (34)) $k_3, k_4, x_3^{\text{ref}}, x_4^{\text{ref}}$ are the same as in Section 3.1.1. Here x_1^{ref} is the desired reference velocity, k_1 is the feedback tracking control gain and has the value $k_1 < 0$. Combining these two controllers enables us to control pitch angle x_4 and velocity x_1 at the same time, provided that the corresponding hidden internal dynamics of the angle of attack x_2 has favourable properties.

3.2.2 Internal dynamics of the angle of attack (x_2): During the design of the controller, the angle of attack x_2 is left uncontrolled.

This corresponds to the hidden uncontrolled internal dynamics. It is essential to check and ensure that this internal dynamics of the angle of attack is stable. Now, to check the stability of the internal dynamics, substitute the expression of control input u_1 (25) and u_2 (33) into the equation of \dot{x}_2 in (13). For simplicity, zero-dynamics are studied. Hence for reference tracking $x_1^{\text{ref}}(t)$, $x_4^{\text{ref}}(t)$, $x_3^{\text{ref}}(t)$ the virtual inputs $v_1 = v_2 = 0$. For purposes of the analysis, constant reference tracking are considered. This means $x_1^{\text{ref}} \equiv x_1^e$, $x_4^{\text{ref}} \equiv x_4^e$, $x_3^{\text{ref}} \equiv 0$ and therefore we have to analyse stability of the equilibrium of the angle of attack's internal dynamics given by

$$\dot{x}_2 = \bar{f}_2(x_2),$$

Here $\bar{f}_2(x_2)$ is given by (55) derived in Appendix 2. To analyse the stability, we have to first compute the equilibrium of the one-dimensional angle of attack by solving (56) and then to analyse the Jacobian of $\bar{f}_2(x_2)$ at x_2^e , i.e. $(\partial \bar{f}_2 / \partial x_2)(x_2^e)$. We will show that $(\partial \bar{f}_2 / \partial x_2)(x_2^e) < 0$ and therefore by the first method of Lyapunov x_2^e is the locally exponentially stable equilibrium of (55). To be more specific, rewrite (56) as follows:

$$\begin{aligned} & b_5 x_1^e (x_1^e) + b_1 b_{13} x_1^e x_2^e x_1^e + (b_4 \cos(x_2^e - x_4^e)) \\ & + (b_8 x_1^e \tan(x_2^e) x_1^e) (b_{14} + b_{15} x_2^e) + \\ & - (b_{10}^{-1} (b_7 + b_2 x_1^e \tan(x_2^e)) (b_4 \sin(x_2^e - x_4^e))) \\ & - (b_{10}^{-1} (b_1 b_{11} x_1^{e2} + b_1 b_{12} x_1^e x_2^e)) = 0. \end{aligned} \quad (35)$$

The above equation can be solved numerically for the equilibrium x_2^e . However, the crucial aspect here is to check that for every selection of x_1^e and x_4^e , the equilibrium solution for x_2^e is within the stall angle range. As a matter of fact, when choosing x_1^e and x_4^e it is important to solve (35) for x_2^e and to ensure that x_2^e is less than stall angle.

To study the local stability of (35) around the equilibrium point $(x_1^e, x_2^e, 0, x_4^e)$, its linear approximation is considered. The partial derivative of (35) (Jacobian), J_{x_2} becomes

$$\dot{x}_1 = J_{x_2} [x_2 - x_2^e] + \mathcal{O}[x_2 - x_2^e]. \quad (36)$$

$$\begin{aligned} J_{x_2} = & b_1 b_{13} x_1^e + b_8 b_{15} x_1^e \tan(x_2^e) \\ & + \frac{(b_2 \sec^2(x_2^e))(b_4 \sin(x_4^e - x_2^e) + b_1 b_{11} x_1^{e2} + b_1 b_{12} x_1^e x_2^e)}{b_{10}} \\ & + \frac{b_4 \sin(x_4^e - x_2^e)}{x_1^e} + (b_8 x_1^e \sec^2(x_2^e))(b_{14} + b_{15} x_2^e) \\ & - \frac{(b_7 + b_2 x_1^e \tan(x_2^e))(b_1 b_{12} x_1^{e2} + b_4 \cos(x_4^e - x_2^e))}{b_{10} x_1^e} \end{aligned} \quad (37)$$

The term

$$\frac{(b_2 \sec^2(x_2^e))(b_4 \sin(x_4^e - x_2^e) + b_1 b_{11} x_1^{e2} + b_1 b_{12} x_1^e x_2^e)}{b_{10}}$$

is related to the drag and engine thrust, hence it is always zero or negative (in practice aircraft cannot fly backward) for any values of x_2^e . The term $b_1 b_{13} x_1^e + b_8 b_{15} x_1^e \tan(x_2^e) < 0$ in (37) for any values of x_2^e . The term $(b_8 x_1^e \sec^2(x_2^e))(b_{14} + b_{15} x_2^e)$ is related to the pitching moment, therefore for $x_2^e > 0$, the term $(b_8 x_1^e \sec^2(x_2^e))(b_{14} + b_{15} x_2^e) > 0$ and for $x_2^e < 0$, $(b_8 x_1^e \sec^2(x_2^e))(b_{14} + b_{15} x_2^e) < 0$. The term

$$\frac{(b_7 + b_2 x_1^e \tan(x_2^e))(b_1 b_{12} x_1^{e2} + b_4 \cos(x_4^e - x_2^e))}{b_{10} x_1^e} < 0$$

is related to the drag, lift, pitching moment produced by the elevator deflection (δe). Hence term

$$\frac{(b_7 + b_2 x_1^e \tan(x_2^e))(b_1 b_{12} x_1^{e2} + b_4 \cos(x_4^e - x_2^e))}{b_{10} x_1^e} > 0$$

for or any values of x_2^e . The condition for J_{x_1} to be negative is (see (38))

The condition in (38) is easily satisfied because the terms on the right hand side are much smaller than the terms on the left hand side. Hence, (36) can be written as

$$\dot{x}_2 = \lambda(x_2 - x_2^e).$$

Here $\lambda = J_{x_2} < 0$. This confirms that the state x_2^e is exponentially stable, i.e. the zero-dynamics of the controller is exponentially stable. It has been shown that for any combination of velocity x_1^e and pitch angle x_4^e the zero-dynamics of the angle of

$$\begin{aligned} u_2 = & \frac{-(b_1 b_{11} x_1^2 + b_1 b_{12} x_2 x_1^2 + b_4 \sin(x_2 - x_4)) b_{10} x_1^2 + (b_8 b_{14} x_1^2 + b_8 b_{15} x_2 x_1^2 + b_9 x_1 x_3) b_2 x_1^2}{(b_3 \cos(x_2))(b_{10} x_1^2)} \\ & + \frac{-b_2 x_1^2 v_1 + b_{10} x_1^2 v_2}{(b_3 \cos(x_2))(b_{10} x_1^2)}. \end{aligned} \quad (33)$$

$$\begin{aligned} u_2 = & \frac{-(b_1 b_{11} x_1^2 + b_1 b_{12} x_2 x_1^2 + b_4 \sin(x_2 - x_4)) b_{10} x_1^2 + (b_8 b_{14} x_1^2 + b_8 b_{15} x_2 x_1^2 + b_9 x_1 x_3) b_2 x_1^2}{(b_3 \cos(x_2))(b_{10} x_1^2)} \\ & - \frac{b_2 x_1^2 (\dot{x}_4^{\text{ref}} + k_3 (x_3 - \dot{x}_4^{\text{ref}}) + k_4 (x_4 - x_4^{\text{ref}})) + b_2 x_1^2 (\dot{x}_1^{\text{ref}} + k_1 (x_1 - x_1^{\text{ref}}))}{(b_3 \cos(x_2))(b_{10} x_1^2)}. \end{aligned} \quad (34)$$

$$\begin{aligned} & \left| \frac{(b_7 + b_2 x_1^e \tan(x_2^e))(b_1 b_{12} x_1^{e2} + b_4 \cos(x_4^e - x_2^e))}{b_{10} x_1^e} \right| + \left| b_1 b_{13} x_1^e + b_8 b_{15} x_1^e \tan(x_2^e) \right| \\ & \left| \frac{(b_2 \sec^2(x_2^e))(b_4 \sin(x_4^e - x_2^e) + b_1 b_{11} x_1^{e2} + b_1 b_{12} x_1^e x_2^e)}{b_{10}} \right| \\ & > \left| (b_8 x_1^e \sec^2(x_2^e))(b_{14} + b_{15} x_2^e) + b_4 \sin(x_4^e - x_2^e) \right|. \end{aligned} \quad (38)$$

attack x_2^e is exponentially stable. However, it is crucial to calculate the equilibrium angle of attack x_2^e and to check that it lies within the operational range to avoid stall.

3.3 Flight controller for angle of attack and velocity (Flight Controller No. 3)

This controller can be used in critical conditions where the aircraft is about to exceeded the stall angle and/or exceeded the maximum construction velocity. A quick automatic recovery controller is needed to bring the angle of attack (x_2) back to a reasonable value. Two crucial tasks in aircraft stall recovery are to get the angle of attack (x_2) within the normal operation range and to control the velocity (x_1) of the aircraft so that it does not fly too fast or too slow. Here the velocity (x_1) is controlled by the engine throttle (u_2), and the angle of attack (x_2) by the elevator deflection (u_1).

3.3.1 Control design. The control objective for this controller is to design a tracking controller for x_2 and x_1 . Thus the auxiliary outputs chosen to get the partial exact feedback linearisation for Flight Controller No. 3, denoted as $h^3(x)$ are as follows:

$$h^3(x) = \begin{bmatrix} x_1 \\ x_2 \end{bmatrix}.$$

Let the virtual inputs to control \dot{x}_2 and \dot{x}_1 be v_1 and v_2 . Lie derivative computation of $h^3(x)$ following (14) and (15) shows that it has the relative degrees $r = (1, 1)$. This gives a two-dimensional internal dynamics. Hence, the feedback linearised form of the system (13) is obtained as follows:

$$\begin{aligned} \dot{x}_1 &= v_2, \\ \dot{x}_2 &= v_1, \end{aligned}$$

The virtual inputs v_1 and v_2 are defined as follows:

$$\begin{bmatrix} v_1 \\ v_2 \end{bmatrix} = \begin{bmatrix} f_2 \\ f_1 \end{bmatrix} + \begin{bmatrix} g_{21} & g_{22} \\ g_{11} & g_{12} \end{bmatrix} \begin{bmatrix} u_1 \\ u_2 \end{bmatrix}. \quad (39)$$

The conditions for the existence of the relative degree as mentioned in (14) and (15) hold if and only if, $x_1 \neq 0$, i.e. for any non-zero velocity of the aircraft. Following (39) the input equations for u_1 and u_2 can be rewritten as follows:

$$\begin{aligned} \begin{bmatrix} u_1 \\ u_2 \end{bmatrix} &= \begin{bmatrix} g_{21} & g_{22} \\ g_{11} & g_{12} \end{bmatrix}^{-1} \begin{bmatrix} f_2 \\ f_1 \end{bmatrix} + \begin{bmatrix} v_1 \\ v_2 \end{bmatrix}. \\ u_1 &= \frac{(b_1 b_{11} x_1^2 + b_1 b_{12} x_2 x_1 + b_4 \sin(x_2 - x_4))(-b_3 x_1^{-1} \sin(x_2))}{(b_3 \cos(x_2))(b_7 x_1) - (b_2 x_1^2)(-b_3 x_1^{-1} \sin(x_2))} \\ &+ \frac{(b_3 \cos(x_2) v_1) - (-b_3 x_1^{-1} \sin(x_2) v_2)}{(b_3 \cos(x_2))(b_7 x_1) - (b_2 x_1^2)(-b_3 x_1^{-1} \sin(x_2))} \\ &- \frac{(b_1 b_5 x_1 + b_1 b_{13} x_2 x_1 + b_6 x_3 + x_3 + b_4 x_1^{-1} \cos(x_2 - x_4)) b_3 \cos(x_2)}{(b_3 \cos(x_2))(b_7 x_1) - (b_2 x_1^2)(-b_3 x_1^{-1} \sin(x_2))}. \end{aligned} \quad (40)$$

$$\begin{aligned} u_2 &= \frac{-(b_1 b_{11} x_1^2 + b_1 b_{12} x_2 x_1 + b_4 \sin(x_2 - x_4)) b_7 x_1}{(b_3 \cos(x_2))(b_7 x_1) - (b_2 x_1^2)(-b_3 x_1^{-1} \sin(x_2))} \\ &+ \frac{-(b_2 x_1^2) v_1 + (b_7 x_1) v_2}{(b_3 \cos(x_2))(b_7 x_1) - (b_2 x_1^2)(-b_3 x_1^{-1} \sin(x_2))} \\ &+ \frac{(b_1 b_5 x_1 + b_1 b_{13} x_2 x_1 + b_6 x_3 + x_3 + b_4 x_1^{-1} \cos(x_2 - x_4)) b_2 x_1^2}{(b_3 \cos(x_2))(b_7 x_1) - (b_2 x_1^2)(-b_3 x_1^{-1} \sin(x_2))} \end{aligned} \quad (41)$$

Combining the two controllers enables us to control the angle of attack (x_2) and the velocity (x_1), provided that the two-dimensional internal dynamics are stable and have favourable properties.

3.3.2 Internal dynamics of pitch rate (x_3) and pitch angle (x_4)

During design of the controller, the pitch rate x_3 and the pitch angle x_4 are left uncontrolled. This corresponds to the hidden uncontrolled internal dynamics. In this controller, the internal dynamics is two dimensional. Now, to checking the internal dynamics, substitute the expression of control input u_1 and u_2 (40) and (41) into the equation of \dot{x}_3 and \dot{x}_4 in (13). For simplicity, zero-dynamics are studied. Hence, for reference tracking $x_1^{\text{ref}}(t)$, $x_2^{\text{ref}}(t)$, the virtual inputs are set to $v_1 = v_2 = 0$. For the purposes of the analysis, constant reference tracking is considered. This means $x_1^{\text{ref}} \equiv x_1^e$, $x_2^{\text{ref}} \equiv x_2^e$. Thus, the equilibrium equation for x_3 and x_4 gets

$$\begin{bmatrix} \dot{x}_3 \\ \dot{x}_4 \end{bmatrix} = \begin{bmatrix} f_3 + (b_{10} x_1^2) u_1 \\ f_4 \end{bmatrix} = \begin{bmatrix} 0 \\ 0 \end{bmatrix}.$$

This can be expanded to give (see Appendix 3 for details of the derivation):

$$\begin{bmatrix} \dot{x}_3 \\ \dot{x}_4 \end{bmatrix} = \begin{pmatrix} \Phi_3 \\ \Phi_4 \end{pmatrix} = 0$$

(see (42))

Here Φ is the internal dynamics function. For every selection of x_1^e and x_2^e , there are unique equilibrium x_3^e and x_4^e such that (42) is zero. For analysing the local stability, we need to analyse the Jacobian of (42). The Jacobian of (42) will be a 2×2 square matrix due to two-dimensional internal dynamics. For the stability proof, we will show that real parts of the eigenvalues of the Jacobian of (42) are negative at the equilibrium.

To study the local stability of (42), its linear approximation around the selected equilibrium points $x = (x_1^e, x_2^e, x_3^e, x_4^e)$ is considered. Here, $x_3^e = 0$ because at the equilibrium pitch angle x_4^e , the pitch rate x_3^e must be zero. The partial derivative of (42) (Jacobian) becomes:

$$\begin{bmatrix} \dot{x}_3 \\ \dot{x}_4 \end{bmatrix} = \begin{bmatrix} \frac{\partial \Phi_3}{\partial x_3} & \frac{\partial \Phi_3}{\partial x_4} \\ \frac{\partial \Phi_4}{\partial x_3} & \frac{\partial \Phi_4}{\partial x_4} \end{bmatrix} \begin{bmatrix} (x_3 - x_3^e) \\ (x_4 - x_4^e) \end{bmatrix}.$$

Thus the Jacobian for \dot{x}_3 and \dot{x}_4 becomes:

$$\frac{\partial \Phi_3}{\partial x_3} = b_9 x_1 - \frac{b_3 b_{10} x_1^2 \cos(x_2) (b_6 + 1)}{b_3 b_7 x_1 \cos(x_2) + b_2 b_3 x_1 \sin(x_2)}, \quad (43)$$

(see (44))

$$\begin{bmatrix} \Phi_3 \\ \Phi_4 \end{bmatrix} = \begin{bmatrix} f_3 + (b_{10} x_1^2) \left(\frac{-(b_1 b_5 x_1 + b_1 b_{13} x_2 x_1 + b_6 x_3 + x_3 + b_4 x_1^{-1} \cos(x_2 - x_4) + (-b_3 x_1^{-1} \sin(x_2)) u_2) + \dot{x}_2^{\text{ref}} + k_2 (x_2 - x_2^{\text{ref}})}{b_7} \right) \\ f_4 \end{bmatrix}. \quad (42)$$

$$\frac{\partial \Phi_4}{\partial x_3} = 1, \quad \frac{\partial \Phi_4}{\partial x_4} = 0. \quad (45)$$

For the stability of the internal dynamics, the roots of the characteristic equation should be negative real roots. The roots of the characteristic equations can be calculated as follows:

$$\left| sI - \begin{bmatrix} \frac{\partial \Phi_3}{\partial x_3} & \frac{\partial \Phi_3}{\partial x_4} \\ \frac{\partial \Phi_4}{\partial x_3} & \frac{\partial \Phi_4}{\partial x_4} \end{bmatrix} \right| = 0.$$

$$s_{1,2} = \frac{(\partial \Phi_3 / \partial x_3) \pm \sqrt{(\partial \Phi_3 / \partial x_3)^2 + 4(\partial \Phi_3 / \partial x_4)}}{2}.$$

Here s is the complex frequency in the Laplace transform. The condition for stability is that the real part of the roots should be negative, i.e.

1. $\partial \Phi_3 / \partial x_3 < 0$ and $\partial \Phi_3 / \partial x_4 < 0$.

Consider $\partial \Phi_3 / \partial x_3$ (43). It can be simplified to:

$$\frac{\partial \Phi_3}{\partial x_3} = b_8 x_1 \left(c_{mac} C_{m_q} - \frac{C_{m_{\delta e}} \cos(x_2) (C_{L_0} + 1)}{b_1 (C_{L_{\delta e}} \cos(x_2) + C_{D_{\delta e}} \sin(x_2))} \right). \quad (46)$$

The term is always $b_8 x_1 > 0$, by definition from (15). The terms C_{m_q} , $C_{m_{\delta e}} < 0$, $C_{L_{\delta e}}$, $C_{D_{\delta e}} > 0$ and $C_{L_0} \geq 0$ by definition. Substituting all these inequalities in (46) gives that $(\partial \Phi_3 / \partial x_3) < 0$.

Now consider the term, $(\partial \Phi_3 / \partial x_4)$ in (44), it can be simplified to give:

$$\frac{\partial \Phi_3}{\partial x_4} = \frac{b_{10} b_4 (b_3 b_4 \cos(x_2 - x_4) \sin(x_2) - b_3 b_4 \sin(x_2 - x_4) \cos(x_2))}{b_3 b_7 \cos(x_2) + b_2 b_3 \sin(x_2)} \quad (47)$$

$$= \frac{b_4 b_{10} (\sin(x_4))}{b_7 \cos(x_2) + b_2 \sin(x_2)}.$$

$$\frac{\partial \Phi_3}{\partial x_4} = \frac{g b_8 C_{m_{\delta e}} \sin(x_4)}{b_1 C_{L_{\delta e}} \cos(x_2) + b_1 C_{D_{\delta e}} \sin(x_2)}. \quad (48)$$

To recover from a stall, the aircraft has to go into a nose dive motion, as such $x_4 < 0$. This implies that the numerator of (48) is always positive due to the term $\sin(x_4)$ being multiplied by $C_{m_{\delta e}} < 0$. The denominator of (48) is also always negative because it is multiplied by the term b_1 which by definition in (15) is negative. It can be therefore be concluded that for this controller $\partial \Phi_3 / \partial x_3 < 0$ and $\partial \Phi_3 / \partial x_4 < 0$. It can be said that the two-dimensional internal dynamics of the proposed controller is stable.

3.4 Controllers gain selection and robustness

It has been shown in Sections 3.1–3.3 that the relation between the virtual inputs and the selected the auxiliary outputs are integral (integrator). Each feedback gains (k_1 , k_2 , k_3 and k_4) can be computed by specifying the time constant of the closed loop. For implementation, flight-handling quality requirements should be taken into account. The flight control system should provide responses satisfying the existing specifications (MIL-STD-1797A and MIL-F-9490D) [21]. Methods for choosing the flight controller gains considering the actuator lag are presented in [22]. While choosing the gain, it is important to make a trade-off between the

response of the controlled variable and the physical actuator's limit, so as not to saturate the control inputs.

The robustness properties of the dynamic inversion have received too little attention in the literature. Some robustness analysis of the NDI controllers is presented in [23, 24]. In [23], authors proposed a sum-of-squared method to analyse the robustness properties of non-linear controller for longitudinal aircraft dynamics. In [24], authors proposed a robust NDI in combination with sliding mode control. Individual studies of each methods are out of scope in this paper. However, to study the basic parametric uncertainties, we have added $\pm 10\%$ uncertainties as an upper bound and lower bound to the nominal values of the controller gains during the simulations (see Section 4).

3.5 Switching of the flight controllers

Flight Controller No.1 can be used for situations like take-off, steady climb of the aircraft when the angle of attack is non-zero. This will allow controlling the aircraft's both angle of attack (α) and pitch angle (θ). For the steady but steep climbing, angle of attack should stay high and singularity at $\alpha = 0$ is not crucial. While using this controller, the velocity of the aircraft will be left uncontrolled. For each combination of angle of attack and pitch angle, there is a stable equilibrium velocity. Difference between the pitch angle and angle of attack is the flight path angle. Hence, this controller can be used for controlling the flight path angle by independently choosing desired angle of attack and pitch angle. For example, for horizontal cruising same tracking values of angle of attack and pitch angle resulting in zero flight path angle.

Using Flight Controller No. 2 velocity and pitch are controlled, while angle of attack is left uncontrolled. This controller can be used for situations where rapid change in pitch up or pitch down manoeuvre is required while having control over the aircraft velocity. Alternatively, this flight controller can be used for faster cruise conditions. For example, assume the aircraft is flying with some reasonable angle of attack using the Flight controller No. 1. Then, for faster cruising, we can set $\theta = x_4 = 0$ and velocity (x_1) to some desired cruising fast velocity to achieve it. In conditions where the angle of attack is critically big (close to stall angle) and the velocity is too slow, Flight Controller No. 3 should be used to get angle of attack within some acceptable range.

Flight Controller No. 3 can be primarily used to recover the aircraft from critical conditions like stall while controlling the velocity while preventing the aircraft from exceeding the maximum construction velocity. The linearising feedback influences of elevator input (u_1) and engine thrust (u_2) on both velocity and angle of attack. Mainly the engine thrust is responsible for controlling the velocity and elevator for controlling the angle of attack. Coupling terms in this controller are smaller, and are rather treated as undesired coupling, which is actually compensated by the linearising feedback. Using this controller, both the angle of attack and the velocity are controlled while leaving pitch angle uncontrolled, which is not very crucial. Indeed, in situations like stall, the 'dangerous' variables are the angle of attack and the velocity. As soon as the aircraft is brought within some acceptable limits of α and velocity the controller can be switched to Flight controller No. 1 or 2.

4 Simulation results and discussion

Simulations are performed with MATLAB/Simulink to verify the proposed controllers on the aircraft model (13). The non-linear aircraft model used for the control design and validation is based on the aerodynamic and flight dynamic data of the F-16 multi-role fighter aircraft (Fig. 3). F-16 is a single-engine supersonic fighter developed by Lockheed Martin for United States Air Force. The physical parameters for the aircraft that are used are as follows [25]: $m = 636.94$ slug, $I_{yy} = 55814$ slugft², $S = 300$ ft²,

$$\frac{\partial \Phi_3}{\partial x_4} = \frac{b_{10} x_1^2 (b_3 b_4 \cos(x_2 - x_4) \sin(x_2) / x_1) - (b_3 b_4 \sin(x_2 - x_4) \cos(x_2) / x_1)}{b_3 b_7 x_1 \cos(x_2) + b_2 b_3 x_1 \sin(x_2)}, \quad (44)$$



Fig. 3 F-16 Fighter Aircraft [26]

$c_{MAC} = 11.32$ ft, $b = 30$ ft. The airfoil used by the F-16 aircraft is NACA 64A-204 and has $\sim 15^\circ$ stall angle [10]. The maximum thrust of the engine (F_T) is 19,000 lbs at the rate limited by $\pm 10,000$ lbs/s. The maximum and minimum elevator deflection (δe) is $\pm 25^\circ$ limited by $60^\circ/s$. The opensource MATLAB/Simulink model used for the demonstration of controller performance verification is found in [26] (https://www.aem.umn.edu/people/faculty/balas/darpa_sec/SEC.Software.html). During the simulation, changes in parameters such as ρ (air density) and ambient air temperature with respect to the altitude were considered to follow International Standard Atmospheric (ISA) condition model. The controller performances are tested using specific manoeuvres. To carry out the robustness analysis, we have considered adding $\pm 10\%$ uncertainty to the nominal values of the controller gains k_1 , k_2 , k_3 and k_4 . For example, if the nominal controller gain value, $k_o = 100$, then the upper bound of the controller gain, $k_{upper} = 110$ and the lower bound of the controller gain, $k_{lower} = 90$.

4.1 Flight Controller No. 1

Flight path angle can be controlled by tracking pitch angle (x_4 or θ) and angle of attack (x_2 or α). To demonstrate the controller performance, the trimmed flight condition were chosen to be at velocity, $V = 550$ ft/s, and altitude 10,000 ft. For demonstrating the controller performance two different manoeuvres were chosen. For the first manoeuvre, pitch angle tracking (x_4) was set to 4° and the angle of attack (x_2) tracking was set to 3° . For the second manoeuvre, x_4 and x_2 tracking were set to -1° and 1° . Both the manoeuvres were set to start from the initial trimmed condition with $x_4 = x_3 = 2.5^\circ$. Following (22) and (24) controller parameters are listed as follows: $k_2 = -60 \text{ s}^{-1}$, $k_3 = -20 \text{ rad s}^{-1}$, and $k_4 = -40 \text{ rad s}^{-2}$. For each manoeuvre the influence of the controller uncertainties are demonstrated. Fig. 4 illustrates the simulation results.

It can be seen that the pitch angle and the angle of attack are exponentially tracked by the controller. In the first manoeuvre, for positive flight path the velocity reduces by exponentially decaying towards 500 ft/s for going against the gravity. However, for controlling the angle of attack with engine thrust, it is essential to provide more thrust to achieve exponential tracking of the angle of attack. In general providing more thrust should increase the velocity, but in the presented case it does not happen because the rate of reduction of velocity (due to pitch of motion) is much larger than the thrust used to control the angle of attack. Hence, irrespective of increasing the thrust to control increase the angle of attack, the decay of velocity decays, but rather slowly.

In the second manoeuvre, a negative flight path angle is demonstrated. It can be seen that the velocity of the aircraft increases and stabilises at around 670 ft/s. At the beginning, higher thrust is required due to large difference between the reference angle of attack and actual angle of attack. However, gradually the thrust requirement settles down.

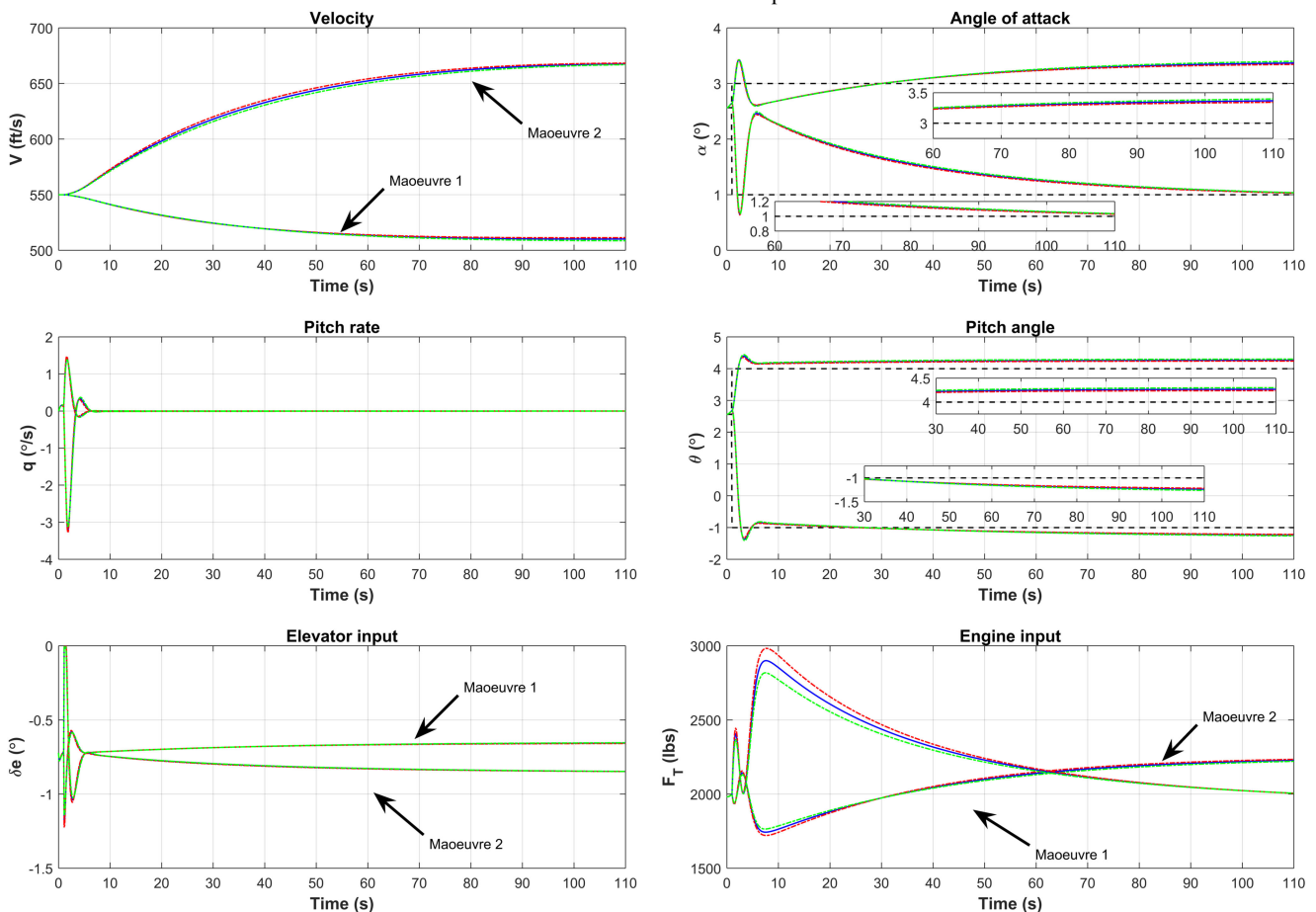


Fig. 4 Angle of attack and pitch angle controller. Blue, red, and green show the controller performance with nominal gains, upper bound gains, and lower bound gains

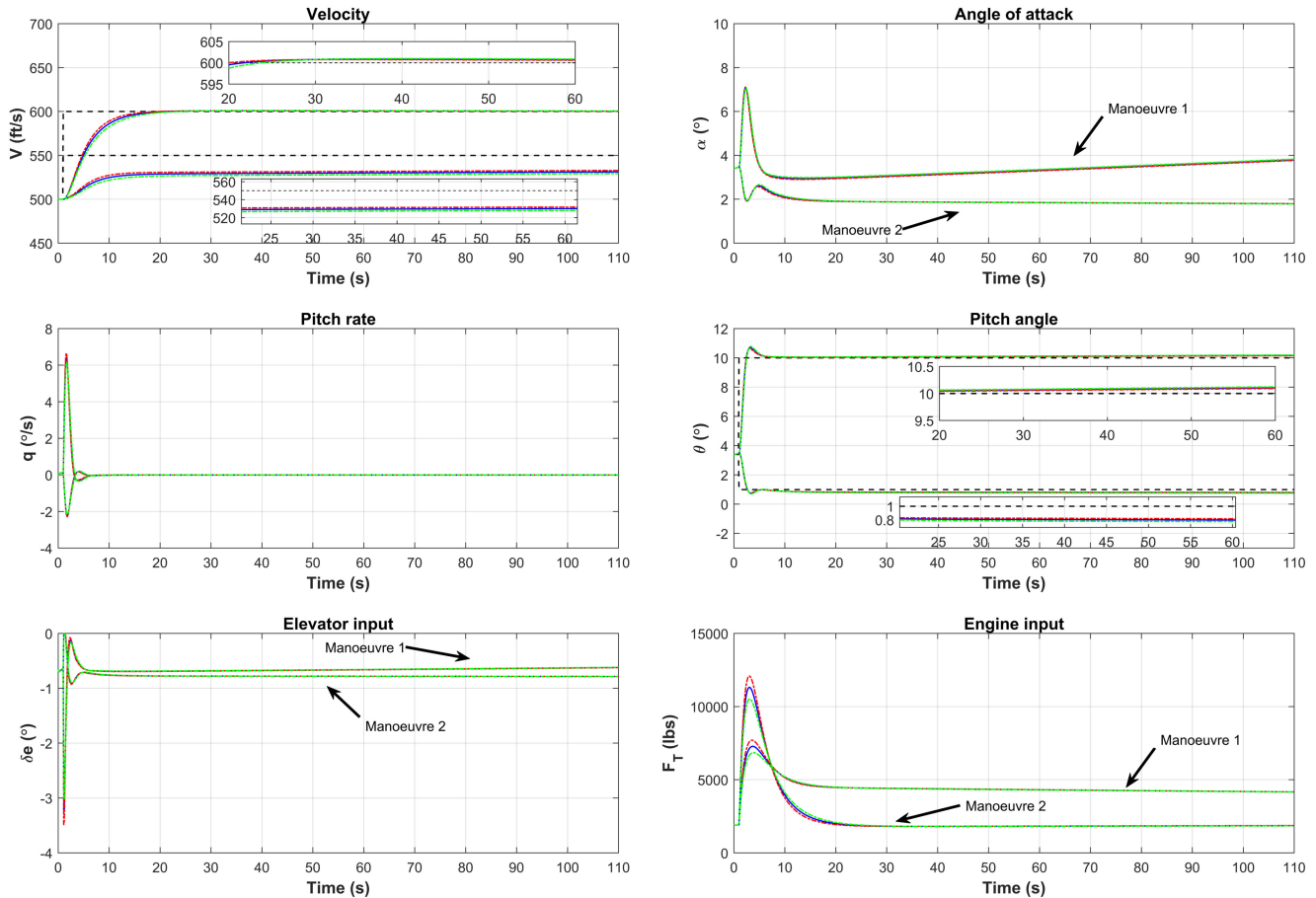


Fig. 5 Pitch angle and velocity controller. Blue, red, and green show the controller performance with nominal gains, upper bound gains, and lower bound gains

To demonstrate the robustness of the control gains, we carried out the simulation of each manoeuvres separately with nominal (blue), upper bound (red), and lower bound (green). For all the cases, the controller exponentially tracked the pitch angle and angle of attack. It is important to notice that for all the cases the uncontrolled velocity stabilises.

4.2 Flight Controller No. 2

To demonstrate the tracking of pitch angle (x_4 or θ) and the velocity (x_1 or V) control, the chosen initial flight condition was cruising velocity of 500 ft/s at an altitude of 10,000 ft. Two different manoeuvres were chosen to show the performance of the controller. Firstly, a nose up motion while tracking the x_4 and x_1 at 10° and 550 ft/s. The second manoeuvre was chosen to be a nose dive motion while tracking the x_4 and x_1 at 1° and 600 ft/s, respectively. Both the manoeuvre initialised from the trimmed condition with $x_4 = 3.4^\circ$. Following (33) and (34), the controller parameters are listed as follows: $k_1 = -100 \text{ s}^{-1}$, $k_3 = -20 \text{ rad s}^{-1}$, and $k_4 = -40 \text{ rad s}^{-2}$. For each manoeuvre, the influence of the controller uncertainties are demonstrated in terms of nominal, upper bound, and lower bound of the controller gains. Fig. 5 illustrates the simulation results.

It can be seen that the velocity V and the pitch angle θ are exponentially tracked. It is noticeable for the pitch down motion (manoeuvre 2), the angle of attack (α) exponentially stabilises at the equilibrium value of 2° . However, for the pitch up motion (manoeuvre 1), the angle of attack stabilised as well but a slower rate. This is because the tracking of velocity while making a pitch up motion is slower. However, it is important to notice the tracking error in pitch angle converges to the zero, and the tracking error for the velocity converges to a small value near zero. The slow convergence of the velocity tracking is due to the chosen controller gains so as not to saturate the engine thrust. To demonstrate the

robustness of the control gains, we carried out the simulation of each manoeuvres separately with nominal (blue), upper bound (red), and lower bound (green). In all the cases, the desired pitch angle and velocity were exponentially tracked.

4.3 Flight Controller No. 3

The performance of the Flight Controller No.3 has been verified assuming the worst case scenario, where the aircraft has reached the stall angle x_2 or $\alpha = 14.87^\circ$ and stall velocity x_1 or $V = 375 \text{ ft/s}$ at an altitude of 30,000 ft. The two important objectives of the controller are: firstly, to bring back the angle of attack of the aircraft within the operating range and secondly, to ensure that the aircraft is not flying too slowly or too fast. Hence, for α and V tracking reference is set to 8° and 550 ft/s. The primary focus of the controller is to get the aircraft out of stall as quick as possible, resulting in vigorous control actions. Following (40) and (41), the controller parameters are listed as follows: $k_2 = -60 \text{ s}^{-1}$ and $k_1 = -86 \text{ rad s}^{-1}$. For the manoeuvre, the influence of the controller uncertainties are demonstrated in terms of nominal, upper bound, and lower bound of the controller gains. Fig. 6 illustrates the simulation performance of the controller.

It can be seen that the angle of attack and the velocity converges to the reference value. It is important to notice that at the start of the manoeuvre the control actions are vigorous and operates at the maximum limits. This is because the high gain values chosen for the tracking controllers of x_1 and x_2 for faster recovery from stall causing maximum control efforts from the actuators (elevator deflection (δe) and thrust (F_T)). It can also be noticed that the pitch rate (q) is exponentially stable and slowly converges to zero. It is important to note that pitch angle (θ) is directly related to pitch rate (q). This residual pitch rate causes a change in the pitch angle (θ) over a long period of time. Here, the controller is only for use in adverse situations, such as stalling. This controller is always in use

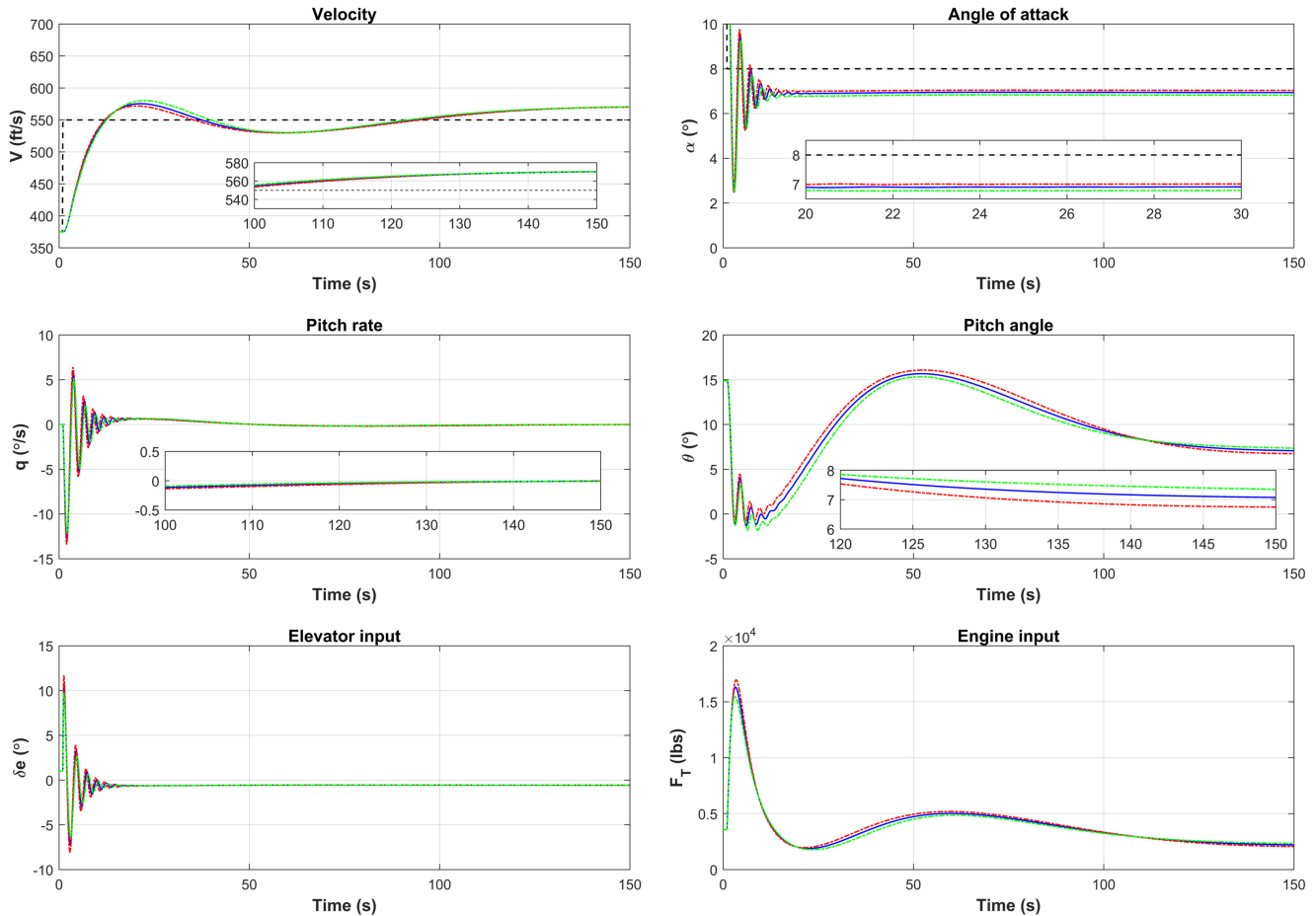


Fig. 6 Angle of attack and velocity controller: Blue, red, and green show the controller performance with nominal gains, upper bound gains, and lower bound gains

for a short duration. Exponential stability of q is not therefore a problem for this controller.

5 Conclusions

In this paper, automatic longitudinal flight controller is presented for conventional fixed-wing aircraft using non-linear dynamic inversion (NDI) technique or, in control theoretic terms, the partial exact feedback linearisation. Main theoretical results include designing of three different tracking flight controllers which provides full control of longitudinal states (velocity, angle of attack and pitch angle) of the aircraft. A detailed study on the stability of the internal dynamics for each controller are carried out and has been showed to be stable. Combination of these three flight controllers depending on the flight condition provided full 3-DOF longitudinal control authority of a fixed-wing aircraft. Simulation results demonstrate that with the proposed controllers, longitudinal motion of a conventional multi-role combat aircraft can be controlled with small tracking error.

6 Acknowledgments

The work of M. Alam was partially supported by the Czech Technical University in Prague under internal grant no. SGS17/137/OHK3/2T/13. The work of S. Celikovskiy was supported by the Czech Science Foundation (GACR) under grant no. 17-04682S.

7 References

[1] Goupil, P.: 'Airbus state of the art and practices on fdi and ftc in flight control system', *Control Eng. Pract.*, 2011, **19**, (6), pp. 524–539
 [2] Anderson, J.D.: 'Fundamentals of aerodynamics' (McGraw Hill, 2007)
 [3] Schroeder, J.A., Burke, R.H.: 'Upset prevention and recovery training—a regulator update'. AIAA Modeling and Simulation Technologies Conf., 2016, pp. 1429

[4] Transportasi, K.N.K.: 'Aircraft accident investigation report'. Ministry of Transportation, Indonesia, Report, 2015
 [5] 'Final Report On the accident on 1st June 2009 to the Airbus A330-203', French Civil Aviation Safety Investigation Authority Std.
 [6] Wise, J., Rio, A., Fedouach, M.: 'What really happened aboard air france 447', *Popular Mech.*, 2011, **6**
 [7] Johnson, E.: 'American Military Transport Aircraft since 1925' (McFarland, 2013)
 [8] Lu, B., Wu, F., Kim, S.: 'Switching l_p control of an f-16 aircraft via controller state reset', *IEEE Trans. Control Syst. Technol.*, 2006, **14**, (2), pp. 267–277
 [9] Santoso, F., Liu, M., Egan, G.: 'H₂ and h_∞ robust autopilot synthesis for longitudinal flight of a special unmanned aerial vehicle: a comparative study', *IET Control Theory Applic.*, 2008, **2**, (7), pp. 583–594
 [10] Stevens, B.L., Lewis, F.L., Johnson, E.N.: 'Aircraft control and simulation: dynamics, controls design, and autonomous systems' (John Wiley & Sons, 2015)
 [11] Lane, S.H., Stengel, R.F.: 'Flight control design using nonlinear inverse dynamics'. American Control Conf., 1986, IEEE, 1986, pp. 587–596
 [12] McLean, D.: 'Globally stable nonlinear flight control system', *IEE Proc. Control Theor. Appl.*, 1983, **130**, (3), pp. 93
 [13] Sieberling, S., Chu, Q., Mulder, J.: 'Robust flight control using incremental nonlinear dynamic inversion and angular acceleration prediction', *J. Guid. Control Dyn.*, 2010, **33**, (6), pp. 1732–1742
 [14] Chen, H., Zhang, S.: 'Robust dynamic inversion flight control law design'. 2nd Int. Symp. on Systems and Control in Aerospace and Astronautics, ISSCAA, IEEE, 2008, pp. 1–6
 [15] Norton, M., Khoo, S., Kouzani, A., et al.: 'Adaptive fuzzy multi-surface sliding control of multiple-input and multiple-output autonomous flight systems', *IET Control Theory Applic.*, 2015, **9**, (4), pp. 587–597
 [16] Khoo, S., Xie, L., Zhao, L.: 'Multi surface sliding control for fast finite time leader follower consensus with high order siso uncertain nonlinear agents', *Int. J. Robust Nonlinear Control*, 2014, **24**, (16), pp. 2368–2404
 [17] Papageorgiou, C., Glover, K.: 'Robustness analysis of nonlinear flight controllers', *J. Guid. Control Dyn.*, 2005, **28**, (4), pp. 639–648
 [18] Reveley, M., Briggs, J., Leone, K., et al.: 'Assessment of the state of the art of flight control technologies as application to adverse conditions (nasa/tm2010-216226)'. NASA TM, 2010, vol. 216226, p. 2010
 [19] Wang, Q., Stengel, R.F.: 'Robust nonlinear flight control of a high-performance aircraft', *IEEE Trans. Control Syst. Technol.*, 2005, **13**, (1), pp. 15–26
 [20] Slotine, J.-J.E., Li, W., et al.: 'Applied nonlinear control' (Prentice-Hall, Englewood Cliffs, NJ, 1991), vol. **199**, no. 1

- [21] Enns, D., Dan, B., Russ, H., *et al.*: 'Dynamic inversion: an evolving methodology for flight control design', *Int. J. Control*, 1994, **59**, (1), pp. 71–91
- [22] Baba, Y., T.L., Sano, M.: 'Design of a nonlinear flight controller based on dynamic inversion'. IEEE Proc. of the 34th SICE Annual Conf. Int. Session Papers, 1995, pp. 1487–1492
- [23] Ataei, A., Qian, W.: 'Non-linear control of an uncertain hypersonic aircraft model using robust sum-of-squares method', *IET Control Theory Applic.*, 2012, **6**, (2), pp. 203–215
- [24] Yang, I., Dongik, L., Dong, H.: 'Designing a robust nonlinear dynamic inversion controller for spacecraft formation flying', *Math. Probl. Eng.*, 2014
- [25] Nguyen, L.T.: 'Simulator study of stall/post-stall characteristics of a fighter airplane with relaxed longitudinal static stability'. National Aeronautics and Space Administration, Technical Report NASA Technical Paper 1538, 1979
- [26] Russell, R.S.: 'Non-linear f-16 simulation using Simulink and Matlab'. University of Minnesota, Technical Paper, 2003

8 Appendix

8.1 Appendix 1: derivation of Flight Controller No. 1

Deriving the equation of the control inputs u_1 and u_2 in the form of $f(x)$ and $g(x)$, we get

$$u_1 = \frac{-f_3 + v_1}{g_{31}}. \quad (49)$$

$$u_2 = \frac{(f_3 - v_1)g_{21}}{g_{22}g_{31}} - \frac{f_2 - v_2}{g_{22}}. \quad (50)$$

Substituting $v_1 = v_2 = 0$, in (49) and (50) we get,

$$u_1 = \frac{-f_3}{g_{31}}, \quad u_2 = \frac{(f_3)g_{21}}{g_{22}g_{31}} - \frac{f_2}{g_{22}}.$$

Now substitute the expression of control input u_1 and u_2 above into the equation of \dot{x}_1 in (13), we get

$$\begin{aligned} \dot{x}_1 &= f_1 + g_{11}u_1 + g_{12}u_2. \\ \dot{x}_1 &= f_1 + g_{11} \frac{-f_3}{g_{31}} + g_{12} \left(\frac{(f_3)g_{21}}{g_{22}g_{31}} - \frac{f_2}{g_{22}} \right) \\ &= f_1 + \left(\frac{g_{12}g_{21}}{g_{22}g_{31}} - \frac{g_{11}}{g_{31}} \right) f_3 - \frac{f_2 g_{12}}{g_{22}}. \end{aligned}$$

$$\frac{g_{12}g_{21}}{g_{22}g_{31}} - \frac{g_{11}}{g_{31}} = \frac{-b_7 \cot(x_2^e) - b_2}{b_{10}}, \quad \frac{g_{12}}{g_{22}} = -x_1^e \cot(x_2^e).$$

$$\frac{g_{12}g_{21}}{g_{22}g_{31}} - \frac{g_{11}}{g_{31}} = \frac{-b_7 \cot(x_2) - b_2}{b_{10}}, \quad \frac{g_{12}}{g_{22}} = -x_1 \cot(x_2).$$

Now substitute $x_3^e = 0$ in the equation of \dot{x}_1 above, we get the internal dynamics as follows:

$$\dot{x}_1 = \bar{f}_1(x_1),$$

Here, (see (51))

$$\begin{aligned} \bar{f}_1 &= ((x_1^e)^2) \left[\cot(x_2^e) \left(b_1 b_5 - \frac{b_7 b_8 b_{14}}{b_{10}} \right) \right. \\ &\quad \left. + x_2^e \cot(x_2^e) \left(b_1 b_{13} - \frac{b_7 b_8 b_{15}}{b_{10}} \right) + b_1 b_{11} + b_1 b_{12} x_2^e \right] \\ &\quad + \left[b_4 \cot(x_2^e) \cos(x_2^e - x_4^e) - \frac{b_2}{b_{10}} (b_2 b_{14} + b_8 b_{15} x_2^e) + b_4 \sin(x_2^e - x_4^e) \right] \end{aligned} \quad (51)$$

$$\frac{g_{22}g_{11}}{g_{12}g_{31}} - \frac{g_{21}}{g_{31}} = \frac{b_2 x_1^e (-b_3 x_1^e \sin(x_2^e))}{b_3 \cos(x_2^e) b_{10} x_1^e} - \frac{b_7 x_1^e}{b_{10} x_1^e} = \frac{-b_3 x_1^e \tan(x_2^e) - b_7}{b_{10} x_1^e}.$$

The equilibrium point of this zero-dynamics (or also equilibrium velocity) x_1^e can be computed solving the following algebraic equation:

$$\bar{f}_1(x_1^e) = 0. \quad (52)$$

8.2 Appendix 2: derivation of Flight Controller No. 2

Deriving the equation of the control inputs u_1 and u_2 in the form of $f(x)$ and $g(x)$, we get

$$u_1 = \frac{-f_3 + v_1}{g_{31}}. \quad (53)$$

$$u_2 = \frac{(f_3 - v_1)g_{11}}{g_{12}g_{31}} - \frac{f_1 - v_2}{g_{12}}. \quad (54)$$

Substituting $v_1 = v_2 = 0$, in (53) and (54) we get,

$$u_1 = \frac{-f_3}{g_{31}}, \quad u_2 = \frac{(f_3)g_{11}}{g_{12}g_{31}} - \frac{f_1}{g_{12}}.$$

Now substitute the expression of control input u_1 and u_2 above into the equation of \dot{x}_2 in (13), we get:

$$\dot{x}_2 = f_2 + g_{21}u_1 + g_{22}u_2$$

$$\begin{aligned} \dot{x}_2 &= f_2 + g_{21} \frac{-f_3}{g_{31}} + g_{22} \left(\frac{(f_3)g_{11}}{g_{12}g_{31}} - \frac{f_1}{g_{12}} \right) \\ &= f_2 + \left(\frac{g_{22}g_{11}}{g_{12}g_{31}} - \frac{g_{21}}{g_{31}} \right) f_3 - \left(\frac{g_{22}}{g_{12}} \right) f_1 \end{aligned}$$

(see equation below)

$$\frac{g_{22}}{g_{12}} = \frac{-b_3 x_1^e \sin(x_2^e)}{b_3 \cos(x_2^e)} = \frac{-\tan(x_2^e)}{x_1^e}.$$

Now substitute $x_3^e = 0$ in the equation of \dot{x}_2 above, we get the internal dynamics as follows:

$$\dot{x}_2 = \bar{f}_2(x_2),$$

here,

$$\begin{aligned} \bar{f}_2(x_2) &= b_1 b_3 x_1^e + b_1 b_{13} x_1^e x_2 + \frac{(b_4 \cos(x_2 - x_4^e))}{x_1^e} \\ &\quad + (b_8 x_1^e \tan(x_2)) (b_{14} + b_{15} x_2) \\ &\quad - \left(\frac{(b_7 + b_2 x_1^e \tan(x_2)) (b_4 \sin(x_2 - x_4^e))}{b_{10} x_1^e} \right) \\ &\quad - \left(\frac{(b_1 b_{11} x_1^e + b_1 b_{12} x_1^e x_2)}{b_{10} x_1^e} \right). \end{aligned} \quad (55)$$

Simplifying the equation above, the equilibrium point of this zero-dynamics (or also equilibrium angle of attack x_2^e can be computed solving the following algebraic equation:

$$\begin{aligned} \bar{f}_2(x_2^e) &= b_1 b_5 x_1^e(x_1^e) + b_1 b_{13} x_1^e x_2^e x_1^e + (b_4 \cos(x_2^e - x_4^e)) \\ &+ (b_8 x_1^e \tan(x_2^e) x_1^e) ((b_{14} + b_{15} x_2^e)) \\ &- (b_{10}^{-1} (b_7 + b_2 x_1^e \tan(x_2^e)) (b_4 \sin(x_2^e - x_4^e))) \\ &- (b_{10}^{-1} (b_1 b_{11} x_1^{e2} + b_1 b_{12} x_1^e x_2^e)) = 0. \end{aligned} \quad (56)$$

8.3 Appendix 3: derivation of Flight Controller No. 3

Deriving the equation of the control inputs u_1 and u_2 in the form of $f(x)$ and $g(x)$, we get

$$u_1 = -\frac{f_2}{g_{21}} - \frac{g_{22}}{g_{21}} u_2 + \frac{v_1}{g_{21}}, \quad u_2 = -\frac{f_1}{g_{12}} - \frac{g_{11}}{g_{12}} u_1 + \frac{v_2}{g_{12}}. \quad (57)$$

$$u_1 = \frac{g_{12}(f_2 - v_1)}{g_{11}g_{22} - g_{12}g_{21}} - \frac{g_{22}(f_1 - v_2)}{g_{11}g_{22} - g_{12}g_{21}}. \quad (58)$$

$$u_2 = \frac{g_{21}(f_1 - v_2)}{g_{11}g_{22} - g_{12}g_{21}} - \frac{g_{11}(f_2 - v_1)}{g_{11}g_{22} - g_{12}g_{21}}. \quad (59)$$

Substituting $v_1 = v_2 = 0$, in (57) and replacing them into the equation of \dot{x}_3 and \dot{x}_4 in (13), we get

$$\begin{bmatrix} \dot{x}_3 \\ \dot{x}_4 \end{bmatrix} = \begin{bmatrix} f_3 + g_{31}u_1 \\ f_4 \end{bmatrix} = \begin{bmatrix} f_3 + (g_{31}) \left(\frac{-f_2 - g_{22}u_2}{g_{21}} \right) \\ f_4 \end{bmatrix}. \quad (60)$$

Now substituting expression for $f(x)$ and $g(x)$ in (60) gives the two-dimensional zero-dynamics:

$$\begin{bmatrix} \dot{x}_3 \\ \dot{x}_4 \end{bmatrix} = \begin{pmatrix} \Phi_3 \\ \Phi_4 \end{pmatrix}$$

(see equation below)

$$\begin{pmatrix} \Phi_3 \\ \Phi_4 \end{pmatrix} = \begin{bmatrix} f_3 + (b_{10} x_1) \left(\frac{-(b_1 b_5 x_1 + b_1 b_{13} x_2 x_1 + b_6 x_3 + x_3 + b_4 x_1^{-1} \cos(x_2 - x_4) + (-b_3 x_1^{-1} \sin(x_2)) u_2) + \dot{x}_2^{\text{ref}} + k_2(x_2 - x_2^{\text{ref}})}{b_7} \right) \\ x_3 \end{bmatrix}.$$